Shot-Noise-Limited Balanced Homodyne Detection for TFLN Squeezing Measurement

Opening

Achieving reliable squeezing measurements on integrated photonic platforms critically depends on operating balanced homodyne detection (BHD) at the shot-noise limit. On 300 nm **thin-film lithium niobate (TFLN)** waveguides with sub-micron mode confinement, however, I find that fiber-to-chip mode mismatch, optical loss, electronic noise, and limitations in the RF readout chain collectively prevent shot-noise-limited operation. These factors degrade the effective detection efficiency and directly suppress observable squeezing.

To address these system-level bottlenecks, I design a co-optimized homodyne detection architecture that integrates **nanophotonic coupling structures, free-space and fiber-based optical interfaces, and wideband low-noise RF readout electronics**, rather than optimizing components in isolation. By explicitly modeling how optical loss, electronic noise, and imperfect common-mode rejection translate into measurable squeezing degradation, I establish a practical pathway toward high-efficiency, quantum-limited homodyne detection for on-chip squeezing experiments.

Objective: Shot-Noise-Limited Balanced Homodyne Detection

Reliable on-chip squeezing measurements require **balanced homodyne detection (BHD) operating at the shot-noise limit**. On 300 nm thin-film lithium niobate (TFLN) platforms, however, I find that fiber-to-chip mode mismatch, optical loss, electronic noise, and imperfect common-mode rejection collectively suppress observable squeezing. To overcome these system-level bottlenecks, I co-design an integrated BHD interface spanning nanophotonic couplers, optical layouts, and wideband RF electronics. I enabled a shot-noise-limited operation with **19.6 dB clearance** and **26 dB CMRR**., 73.4% quantum efficienct. A 97% quantum efficiency module is under characterization.

Loss-Induced Squeezing Degradation

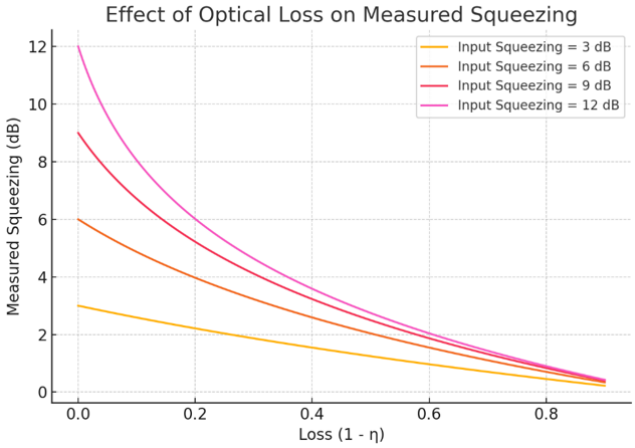

η is the overall effective detection efficiency

$$\eta = \eta_{\text{coupling}} \times \eta_{\text{QE}}$$

Optical loss mixes vacuum noise and suppresses measurable squeezing

$$< X_{out}^2 > \ = \eta < X_s^2 > + (1-\eta) < X_{vac}^2 >$$

$$V_{out} = \eta V_{in} + (1-\eta)$$

1. Balanced Homodyne Detection Interface with Taper Design

1.1 Fiber Couple Detector Analysis

- **Detector Quantum Efficiency (η_{QE}):**
  - **PDB770C:** 73.4%
  - **BDXQ1F:** 97%

However, I identify chip-to-fiber coupling (η_coupling) as the dominant bottleneck limiting total detection efficiency. To address this, I design an **edge-lens coupler for our 300 nm TFLN waveguide**, achieving **65% coupling efficiency** to a lensed fiber with 2.5 μm mode diameter (product of transmission and mode overlap).

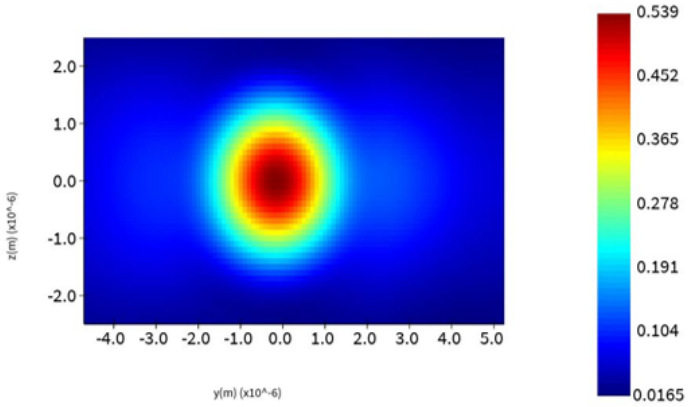

2. Free Space Detection Analysis

I also explore free-space coupling as an alternative interface. The small vertical mode size of the 300 nm TFLN waveguide limits collection efficiency with standard optics (NA = 0.85). In comparison, a 500 nm platform supports a larger mode and achieves 70% coupling (reported in literature), while the 300 nm device yields only ~49%.*

Waveguide Structure	300 nm Waveguide	500 nm Waveguide
Rib Height	$120\ \mathrm{nm}$	$300\ \mathrm{nm}$
Slab Height	$180\ \mathrm{nm}$	$200\ \mathrm{nm}$
Lens NA	0.85	0.85
Coupling Efficiency	49%	70% (reported in the paper)

$$\eta_x = 1 - exp(-2 \times (\frac{tan(\theta_{lens})}{tan(\theta_{beam,x})})^2) \approx 49\%$$

Free Space BHD Optical Layout

To improve this, I design tapers that expand the mode diameter beyond 1 μm (current simulation target: 2.5 μm). If fabricated successfully, such modes would enable >90% free-space coupling.

For the current setup, I optimize the optical layout to minimize loss:

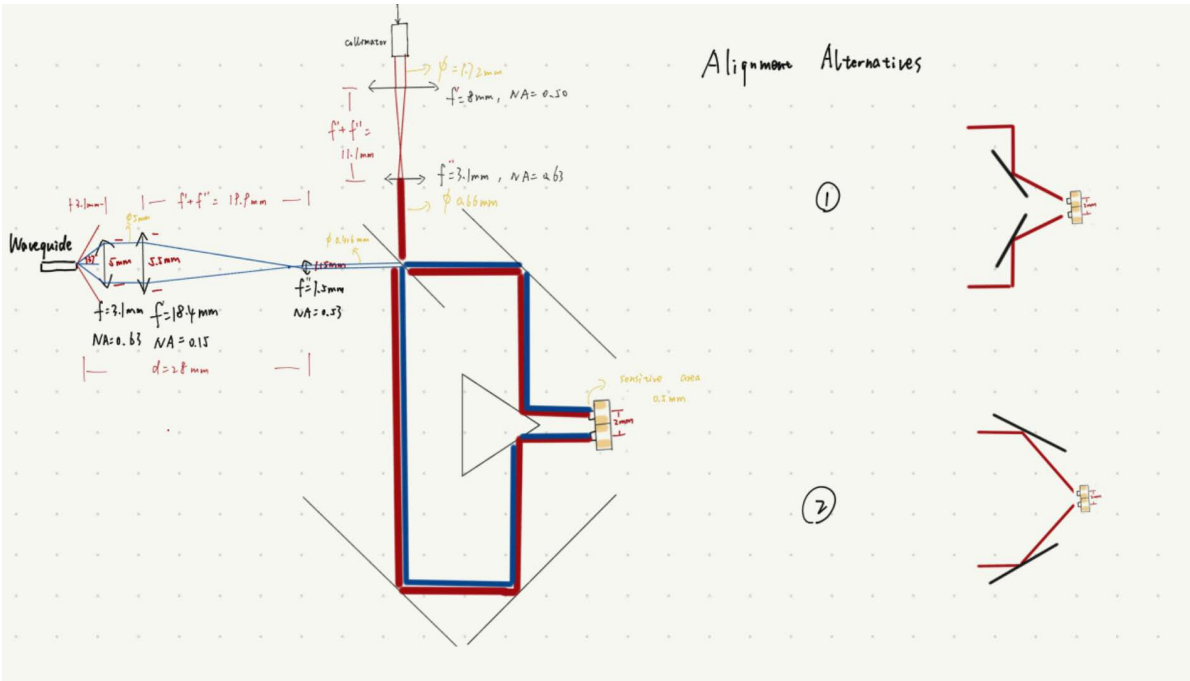

- **Squeezed Light:** Collimated to $5\ \mathrm{mm}$ diameter, then reduced via $4f$ system to $0.416\ \mathrm{mm}$.
- **LO Light:** Collimated to $1.72\ \mathrm{mm}$, reduced to $0.66\ \mathrm{mm}$ to fully cover the signal beam.

By combining this layout with high-QE photodiodes, I project a **total detection efficiency exceeding 80%** for the free-space interface..**

I have also **developed the PCB Layout in KiCad** to support the impedance matching.

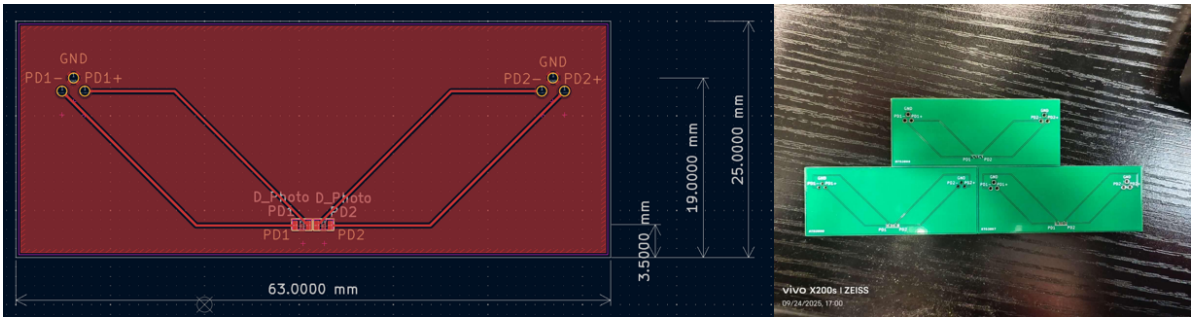

2. Fiber-to-Chip Coupling: Edge Coupler Modeling and Optimization

2.1 Edge-Lens Coupler Design on 300 nm LN waveguide (no slab)

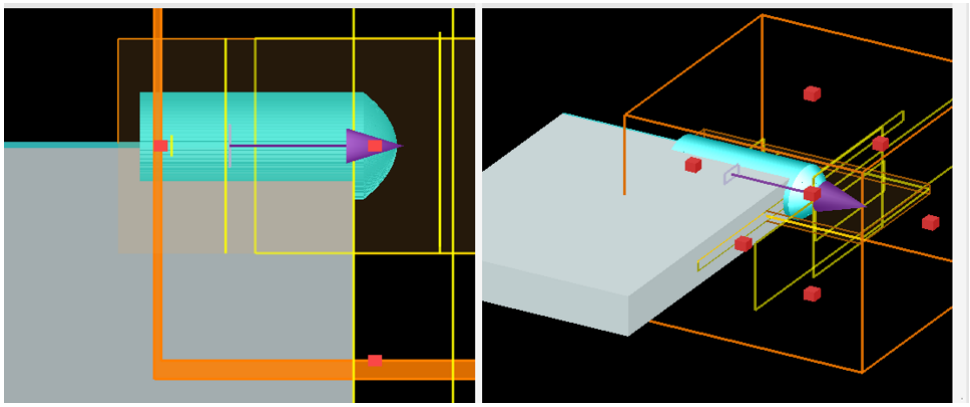

I designed lens coupler (refractive index = 1.63): written on top of the TFLN waveguide facet

Custom even-order aspheric edge-lens: geometry is defined by an even-order radial polynomial, up to the fourth order

$$h(r) = c_0 + c_2 \cdot 10^3 \cdot r^2 + c_4 \cdot 10^9 \cdot r^4$$

Geometric parameters: lens curvature, radius, axial offset

Coupling target: Lensed fiber with Gaussian mode Mode size: 2.5 μm diameter, $1/e^2$

2.2 Mode Overlap Calculation with Mode Center Bias

- Due to typical offset of the mode from the geometric center, I compute the actual waveguide mode center using custom code
- A Gaussian fiber mode (2.5 μm diameter, 1/e²) is then centered at this position to compute the accurate mode overlap.

2.3 Elliptical Asphere Design on 300 nm Squeezing LN Waveguide (120 nm slab)

Due to lateral mode expansion from rib width reduction, circular lenses cannot simultaneously optimize beam shaping in both transverse directions.

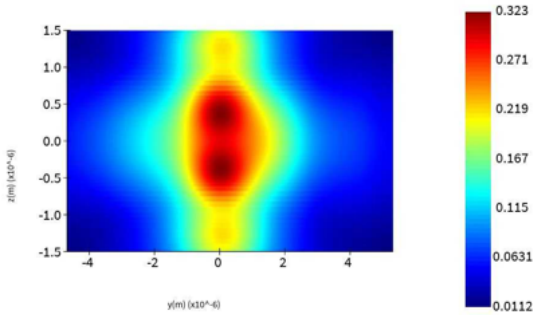

To resolve this, I design an **elliptical aspheric edge-lens**, enabling independent control over x and y divergence. My optimization targets maximum effective coupling efficiency:

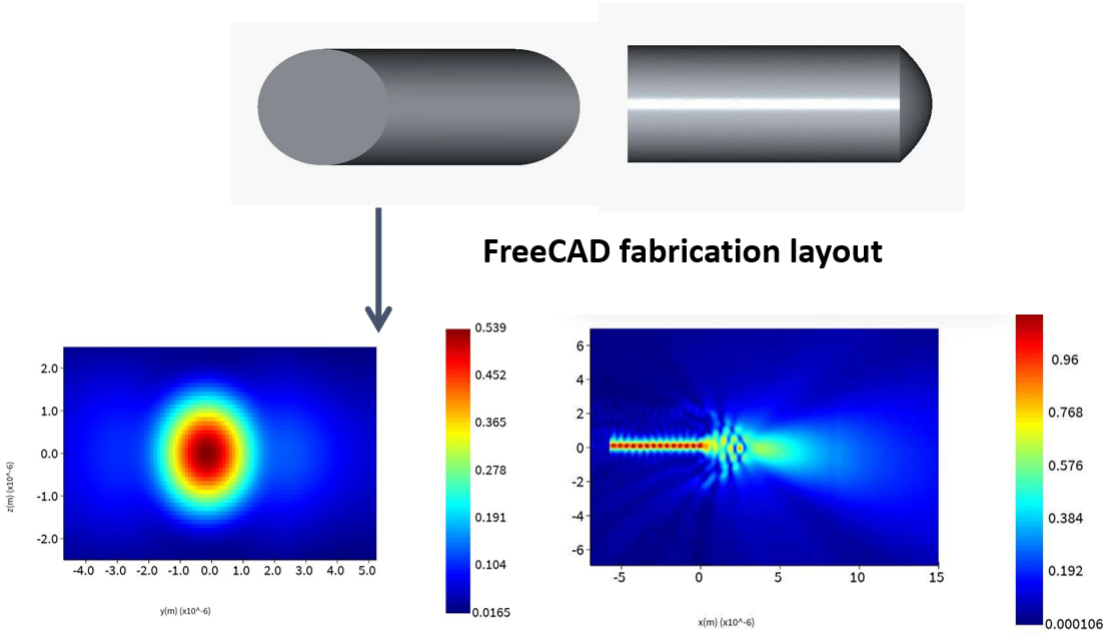

Target: maximized effective coupling efficiency

$$\eta_{total} = \eta_{geom} \times \eta_{overlap}$$

η_{geom}: geometrical transmission

$\eta_{overlap}$: mode-overlap efficiency

Through optimization, I achieved **a total coupling loss of 1.8 dB per facet** for rib TFLN waveguide.

3. Wideband RF Balanced Detector Assembly and Shot-Noise Characterization

3.1 Results Summary

Parameter	Characterization Result
Shot Noise Clearance Ratio	**19.61 dB @ 10 dBm**
Responsivity	**0.917 A/W (Data Sheet Curve: 0.89 A/W)**
Quantum Efficiency from Measured Responsivity	**73.4%**
CMRR	**26.36 dB**
NEP (RF Electronic Noise Floor)	**8.6 pW/$\sqrt{Hz}$**
Shot noise linear fit R^2	**0.9967**
Monitor Balance	**below 0.2% difference**
Monitor Offset	**0-1mV**

3.2 Low Inductance Electronic Interface for PDB770C & BDXQ1F

3.2.1 Thermal management + Electrostatic Discharge (ESD) protection

I limited **solder contact to <4 s**, and allowed **>10 s of cooling time** between joints.

3.2.2 Millimeter-scale castellated edge pads micro-soldering.

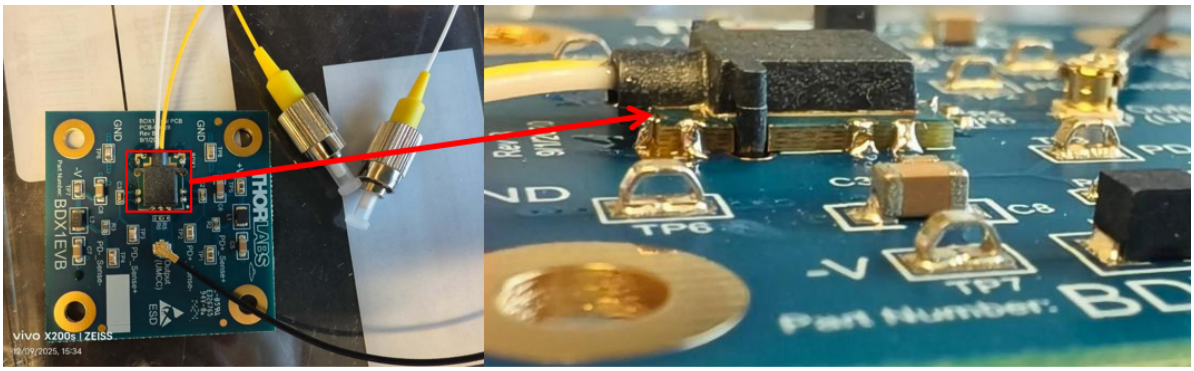

3.3 Power-On characterization

Noise Equivalent Power (NEP) - RF noise floor:

$$\mathrm{NEP} \approx 8.57 \times 10^{-12}\ \mathrm{W}/\sqrt{\mathrm{Hz}}$$

$$Minimum\ \mathrm{NEP}\ from\ spec\ sheet = 8 \times 10^{-12}\ \mathrm{W}/\sqrt{\mathrm{Hz}}\ (DC\ -\ 100\ MHz))$$

This result validates the effective suppression of the electronic dark noise floor ($\mathrm{NEP} \approx 8.57\ \mathrm{pW}/\sqrt{\mathrm{Hz}}$). The shot noise is the dominant contribution to the signal.

Shot Noise Limit (SNL) and System Efficiency

All of the input power were measured by an optical power meter.

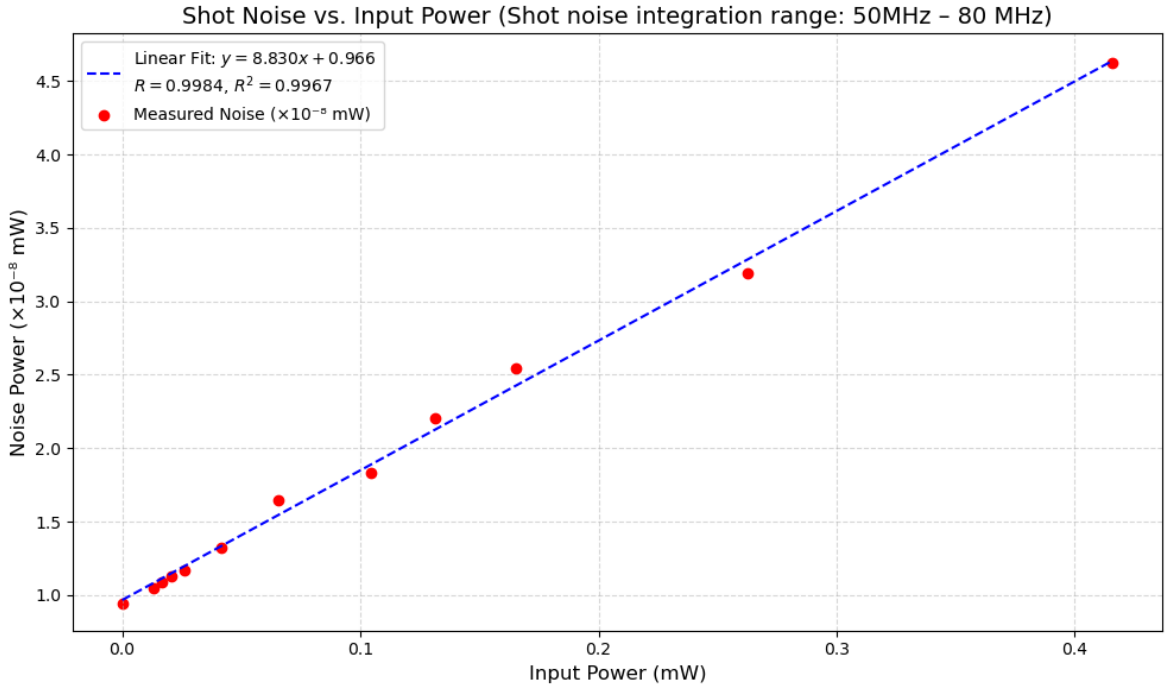

Under illumination, the RF noise scales linearly with optical power (R^2 = 0.9967), confirming shot-noise-limited operation. From the responsivity (**0.917 A/W**), I extract an effective quantum efficiency of **73.4%**. These results confirms operation deep in the **shot-noise-limited regime.**

4. Common mode rejection ratio (CMRR)

Local oscillator intensity noise (RIN) generates excess current noise $S_I^{\text{excess}} = RIN \times I^2$. In an ideal balanced homodyne detection (BHD) setup, differential detection cancels this common-mode noise. However, due to finite common-mode rejection ratio (CMRR), a residual component remains. I measure a **CMRR of 26.36 dB** (linear ratio ≈ 433), sufficient to suppress RIN below the shot-noise floor.

$$\text{CMRR}_{\text{linear}} = \frac{\text{Input Common Mode Noise } (S_I^{\text{excess}})}{\text{Residual Differential Output Noise } (S_I^{\text{excess, residual}})} \approx 433$$

$$\text{CMRR (dB)} = 10 \cdot \log_{10}(433) \approx 26.36 \text{ dB}$$

CMRR Conclusion

This result demonstrates that the system's **common-mode noise is** effectively suppressed, leaving minimal residual excess noise in the **differential** RF **signal**, and the system performance is fundamentally limited by **quantum shot noise**.

Conclusion and Outlook

In this work, I demonstrate a shot-noise-limited balanced homodyne detection platform tailored to thin-film lithium niobate squeezing experiments. I identify optical coupling loss, not photodiode quantum efficiency, as the dominant limitation on overall detection efficiency. Guided by this insight, I design and optimize inverse tapers and aspheric edge-lens couplers using full 3D electromagnetic simulations, achieving **1.8 dB per-facet coupling loss** and establishing a clear path toward further improvement.

On the detection side, I implement a wideband, low-noise RF readout chain, achieving **19.6 dB shot-noise clearance**, **73.4% effective quantum efficiency**, and **26.4 dB common-mode rejection**. The linear dependence of noise on optical power ($R^2 = 0.9967$) confirms operation deep in the shot-noise-limited regime, and the close agreement with theory validates both modeling and implementation.

Together, these results prove that **quantum-limited homodyne detection on sub-micron TFLN platforms is achievable** through coordinated co-design of photonic interfaces, optical layouts, and RF electronics. The methodologies I develop—particularly coupling-aware efficiency analysis and integrated opto-electronic optimization—are directly extensible to next-generation on-chip squeezing sources and quantum transduction experiments, where maximizing detection efficiency is essential for observing nonclassical states.